IOP Conf. Series: Materials Science and Engineering **724** (2020) 012025 doi:10.1088/1757-899X/724/1/012025

Surface roughness influence on active surfaces geometry and modified rating life of rolling contacts

M Benchea[1] **and S Crețu**[1]

[1]Mechanical Engineering, Mechatronics and Robotics Department, "Gheorghe Asachi" Technical University of Iaşi, Iaşi, Romania

E-mail: marcelin.benchea@tuiasi.ro

Abstract. The active surfaces topography of bodies in rolling contact can be obtained by different manufacturing technology. The scope of this paper is to evidence the influence of the initial surface roughness on running-in process, working surface geometry and durability of rolling contacts. The paper presents a numerical study applied on a toroidal roller bearing where the modified rating lives have been evaluated with the methodologies mentioned by ISO 16281.

1. Introduction

The topography of the active surfaces in rolling contact depends on the surface manufacturing process technology. In the field of engineering the exact degree of roughness can be of considerable importance, affecting the function of a component or its cost [1,2,3].

The roughness of the surfaces that interacts has an important role on its tribological behaviour. The solutions of the models used in order to describe it [4,5] require the input of a three-dimensional rough profile. Since the experimental acquisition of such profiles does not allow a sufficiently large sample of profiles to be used, an essential requirement for any numerical algorithm is to generate arbitrarily rough surfaces with the same or similar proprieties of the real surfaces [6,7].

When two engineering surfaces are loaded for the first time changes in the topography of both surfaces generally occur. These changes appear between start-up and steady state and are associated with running-in process [8,9].

An analysis model was developed to model the nonlinear strain rate dependent deformation of materials stressed in elastic-plastic domain [10,11]. The model is developed in the frame of incremental theory of plasticity using the von Mises yield criterion and Prandtl-Reuss equations. Considering the isotropic and non-linear kinematic hardening laws of Lemaitre-Chaboche [12,13] the model accounts for the cyclic hardening phenomena.

The nano-asperities of contact surfaces generate high pressure peaks in pressure distributions that can severely diminish the modified rating life as is defined by [14].

2. Theory

2.1. Elastic-plastic model

The elastic-plastic model developed to evaluate the plastic deformation of the surfaces considers the material cyclic hardening characteristic that is described by a combined isotropic and nonlinear kinematic hardening laws [12,13].

The yield surface is defined by the von Mises yield criterion:

$$F = f(\sigma - \alpha) - \sigma_Y^0 = 0 \tag{1}$$

where $f(\sigma - \alpha)$ is the equivalent von Mises stress and σ_Y^0 is the yielding stress.

The non-linear kinematic hardening component describes the ratchetting effect by expressing the translation of the yield surface in the stress space through the back-stress α.

The isotropic hardening component of the model defines the yielding stress as a function of the equivalent plastic strain and is given by the relation:

$$\sigma_Y^0 = \sigma_{Y0} + Q_\infty \cdot \left(1 - e^{-b_\infty \cdot \bar{\varepsilon}^p}\right) \tag{2}$$

where Q_∞ is the limiting change in the yield surface size on the deviatoric plane and b_∞ describes how rapid the limit size is reached [15].

According to the energetic theory of fracture, the von Mises stress is an equivalent uniaxial traction stress [13]. For a 3D contact loading in each point of the stressed volume the equation of von Mises stress amplitude includes all 6 components of the stress tensor. For this consideration, when the yield limit is overcome, it can be used the pseudo-plastic Ramberg-Osgood's equation in the combined hardening laws, equation that gives the correspondence between the intensity of the stress tensor and the intensity of the strain tensor:

$$\bar{\varepsilon}_e = \frac{\bar{\sigma}_e}{E} + \left(\frac{\bar{\sigma}_e}{B}\right)^N \tag{3}$$

where B is the coefficient of plastic resistance and N is the hardening exponent [10,11].

The plastic deformation of the surfaces is given by the plastic strains accumulated in the sub-surface layer:

$$u^p(x,y) = \int_0^z \varepsilon^p(x,y,z) \cdot dz \tag{4}$$

2.2. Modified rating life

The classic computation of the rolling bearings basic rating life considers only the equivalent load on the bearing P, dynamic capacity load C and an exponent p depending of the rolling element:

$$L_{10} = \left[\frac{C}{P}\right]^p \tag{5}$$

where $p = 3$ for ball bearings and $p = 10/3$ for roller bearings [16].

To take into account the peaks of the pressure distributions generated by the presence of the nano-asperities on the surface, was developed a method to compute the basic rating life with methodology given by the standard ISO 16281 [14].

In the first instance, for the roller bearings, to evaluate the rating life is needed to determine the elastic deflection of each loaded roller j that depends on the radial load and internal radial clearance of the bearing:

$$\delta_j = \delta_r \cdot \cos\varphi_j - \frac{s}{2} \tag{6}$$

In the second instance, to consider de load on every loaded roller is used the lamina model as is described in [14] and the roller is divided into n_s identical laminae.

The load $q_{j,k}$ on lamina k of the roller j is:

$$q_{j,k} = c_s \cdot \delta_{j,k}^{10/9} \tag{7}$$

with the spring constant c_s:

$$c_s = \frac{35948 \cdot L_w^{8/9}}{n_s} \tag{8}$$

were L_w is the roller length and n_s is the laminae number [14].

In the third instance, the basic rating life L_{10r} of the roller bearings is calculated with:

$$L_{10r} = \left\{ \sum_{k=1}^{n_s} \left[\left(\frac{q_{kci}}{q_{kei}} \right)^{-9/2} + \left(\frac{q_{kce}}{q_{kee}} \right)^{-9/2} \right] \right\}^{-8/9} \tag{9}$$

where: q_{kci} - basic dynamic load rating of a bearing lamina of the inner ring,
q_{kce} - basic dynamic load rating of a bearing lamina of the outer ring,
q_{kei} - dynamic equivalent load on a lamina k of a rotating inner ring,
q_{kee} - dynamic equivalent load on a lamina k of a stationary outer ring.

According to standard [14], the dynamic equivalent loads on each lamina of the inner/outer ring q_{kei} and q_{kee} are computed as a function of the stress riser coefficients evaluated for each lamina of each roller. The stress risers are calculated considering the pressure distribution on the corresponding lamina.

In the last instance, the modified rating life L_{10mr} of the roller bearings is given by:

$$L_{10mr} = \left(\sum_{k=1}^{n_s} \left\{ \left[a_{ISO} \left(\frac{\eta_c \cdot P_u}{P_{ks}}, \kappa \right) \right]^{-9/8} \cdot \left[\left(\frac{q_{kci}}{q_{kei}} \right)^{-9/2} + \left(\frac{q_{kce}}{q_{kee}} \right)^{-9/2} \right] \right\} \right)^{-8/9} \tag{10}$$

where the life modification factor a_{ISO} is calculated for each bearing lamina k using its dynamic equivalent load P_{ks}:

$$P_{ks} = 0.323 \cdot Z \cdot n_s \cdot \cos\alpha \cdot \left[\frac{q_{kei}^{9/2} + \left(1.038 \cdot q_{kci}/q_{kce}\right)^{9/2} \cdot q_{kee}^{9/2}}{1 + \left(1.038 \cdot q_{kci}/q_{kce}\right)^{9/2}} \right]^{2/9} \tag{11}$$

In facts, the life modification factor a_{ISO} is a function that depends on the lubrication factor κ, oil contamination factor η_c and fatigue load limit P_u for the given application [16].

3. Results and Discussion

A toroidal roller bearing - CARB C2318, has been selected for the numerical case study. The main geometrical data are as follows: inner ring diameter $d_{ci} = 115$ *mm*, outer ring diameter $d_{ce} = 165$ *mm*, roller diameter $d_w = 25$ *mm*, roller length $L_w = 54$ *mm*, number of rollers $Z = 14$. The catalogue data [17]: dynamic capacity load $C = 610$ *kN* and fatigue load limit $P_u = 73.5$ *kN*.

For numerical case study of the running-in process a medium radial loading $F_R = 0.185 \cdot C = 112.5$ *kN* and three magnitudes of the surface roughness parameters was used: a fine roughness with $R_{qw1} = 40$ *nm* for roller surface and $R_{qi1} = 70$ *nm* for inner ring raceway surface, similar to the surface roughness values measured with Taylor Hobson profilometer, a medium roughness with $R_{qw2} = 80$ *nm* and $R_{qi2} = 140$ *nm* and a grossly roughness with $R_{qw3} = 120$ *nm* and $R_{qi3} = 210$ *nm*.

To consider the material behaviour, in the elastic-plastic model was used the following parameters of the roller bearing steel: the Young modulus $E = 209\ GPa$, the Poisson coefficient $v = 0.29$, the yielding stress $\sigma_{Y0} = 1650\ MPa$, the limiting change in the yield surface size on the deviatoric plane $Q_\infty = -100\ MPa$ and $b_\infty = 120$ which describes how rapid the limit size is reached [15], the coefficient of plastic resistance $B = 4320\ MPa$ and the hardening exponent $N = 12.6$ [10,11].

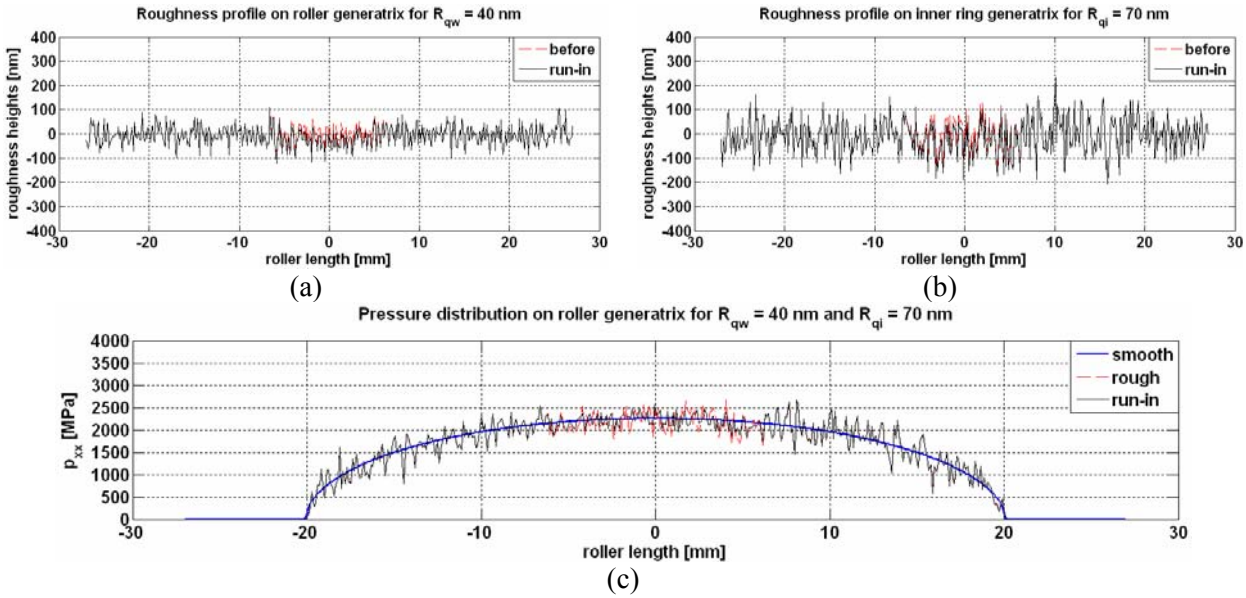

Figure 1. Numerical results for highest loaded roller-inner ring contact ($R_{qw1} = 40\ nm$, $R_{qi1} = 70\ nm$): (a) roughness profile on roller (before and after run-in), (b) roughness profile on inner ring (before and after run-in) and (c) pressure distribution.

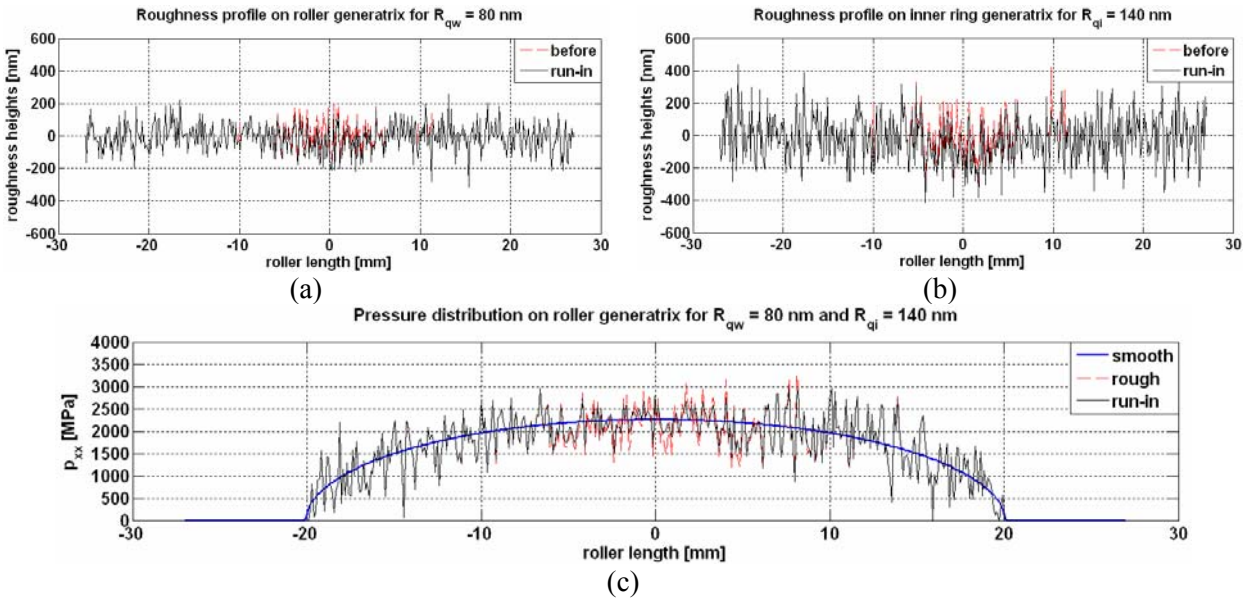

Figure 2. Numerical results for highest loaded roller-inner ring contact ($R_{qw1} = 80\ nm$, $R_{qi1} = 140\ nm$): (a) roughness profile on roller (before and after run-in), (b) roughness profile on inner ring (before and after run-in) and (c) pressure distribution.

In figures 1(a),(b), 2(a),(b) and 3(a),(b) are presented the 2D roller and inner ring roughness profiles before and after *300* running cycles. It can be observed that the running-in process is more pronounced for the inner ring and the roughness heights are plastic deformed in the middle contact

area for *10 mm* in length for R_{qi1} = *70 nm*, for *20 mm* in length for R_{qi2} = *140 nm* and for *40 mm* in length for R_{qi3} = *210 nm*. The plastic deformations of the roughness peaks are higher as the roughness is coarser.

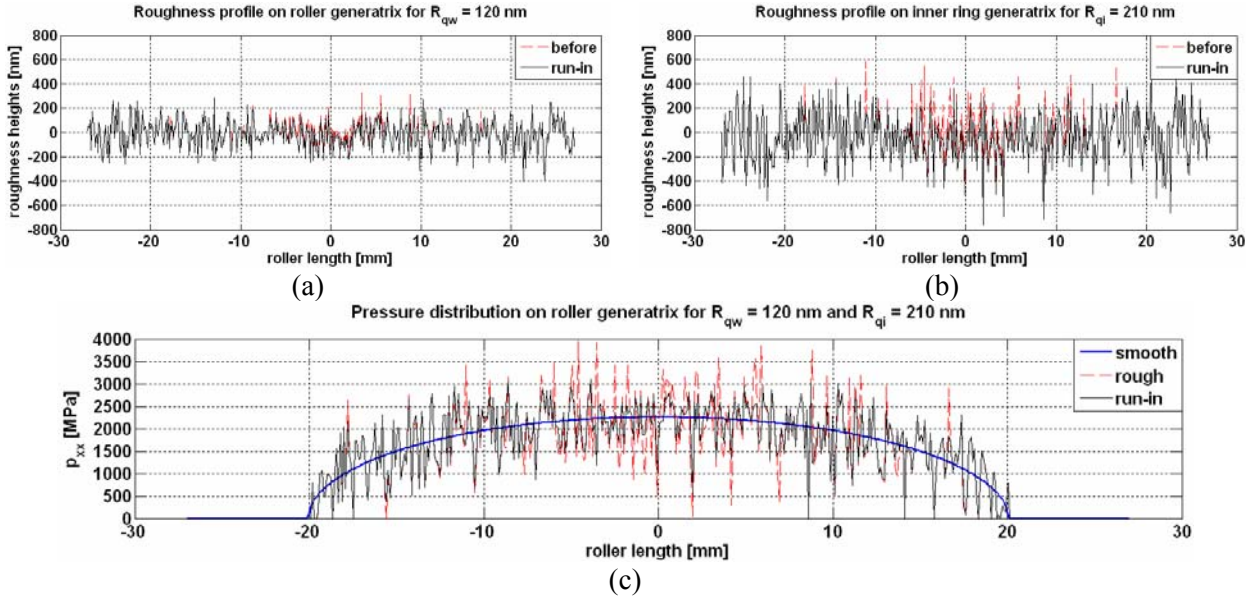

Figure 3. Numerical results for highest loaded roller-inner ring contact (R_{qw1} = *120 nm*, R_{qi1} = *210 nm*): (a) roughness profile on roller (before and after run-in), (b) roughness profile on inner ring (before and after run-in) and (c) pressure distribution.

The 2D pressure distributions on roller generatrix for the highest loaded roller-inner ring contact are presented in figures 1(c), 2(c) and 3(c). In comparison with a smooth contact surface it can be observed that the presence of the roughness on the contact surface generates peaks in pressure distributions. The pressure peaks are higher as the roughness is more grossly and have the maximum value of *2700 MPa* for the fine roughness, *3200 MPa* for the medium roughness and *4000 MPa* for the grossly roughness. In the middle of the contact length the maximum pressure for the smooth contact surface is *2250 MPa*.

It can be observed that after *300* running cycles the pressure peaks are slightly diminished in the middle of the contact length for the fine and medium roughness and are significantly diminished on the all contact length for the grossly roughness.

Table 1. Rating lives for light loading conditions (F_R = *0.055·C = 33.5 kN*)

Roller roughness R_{qw} [*nm*]	Inner ring roughness R_{qi} [*nm*]	Rating life, L_{10}, *hours*, [16]	Modified rating life, L_{10mr}, *hours*, [14]	
			Before	Run-in
smooth	smooth	*264700*	*688750*	
40	*70*		*218660*	*324140*
80	*140*		*28205*	*74993*
120	*210*		*2297*	*38602*

In table 1 are presented the modified lives L_{10mr} for light loading conditions (F_R=*0.055·C=33.5kN*). The values of the modified rating life are smaller for the rough surfaces than for the smooth surface. For the case of modified surfaces after *300* running cycles with medium radial loading, it can be

observed an increase of the modified rating life, apparently a higher increase for the grossly roughness, approximately *16* times more than before run-in (from *2297 hours* to *38602 hours*), but a significantly increase for the fine roughness, approximately *105000 hours* more than before run-in (from *218660 hours* to *324140 hours*).

4. Conclusions

The topography of the active surfaces in rolling contact depends on the surface manufacturing process technology. Numerical results presented in this paper evidence the fact that the presence of nano-asperities on contact surfaces influence the running-in process and durability of rolling contacts.

It was used a numerical method to generate an arbitrarily defined three-dimensional rough surface, a elastic-plastic model to take into account the running-in process and the new methodology given by ISO 16281 to evaluate the modified rating life.

The presence of nano-asperities on contact surfaces generates peaks in pressure distributions, higher peaks for surfaces with grossly roughness. For surfaces with coarser roughness the running-in process is more pronounced than for surfaces with a finer roughness.

The modified rating life it is severely diminished for surfaces with coarser roughness (by two orders of magnitude), even after running-in process (by one order of magnitude) than for smooth surfaces or with a finer roughness.

5. References

[1] Robbe-Valloire F 2001 Statistical analysis of asperities on a rough surface *Wear* **249** pp 401-408
[2] Taylor Hobson Precision 2003 *Exploring surface texture* (TH Ltd)
[3] Stawicki T, Sedlak P, Koniuszy A 2010 The testing of the influence of the roughness of the crankshaft journal upon the durability of the crankshaft bearing in engines of agricultural machines *Sci. probl. of mach. op. and maint.* **4** pp 7-17
[4] Allwood J, Ciftci H 2005 An incremental solution method for rough contact problems *Wear* **258** pp 1601-1615
[5] Allwood J 2005 Survey and performance assessment of solution methods for elastic rough contact problems *J. Tribol.* **127** pp 10-23
[6] Bakolas V 2003 Numerical generation of arbitrarily oriented non-gaussian three-dimensional rough surfaces *Wear* **254** pp 546-554
[7] Patrikar RM 2004 Modeling and simulation of surface roughness *App. Surf. Sci.* **228** pp 213-220
[8] Jamari J 2006 *Running-in of rolling contacts* (PhD Thesis Twente)
[9] Jamari J, de Rooij MB and Schipper DJ 2007 Plastic deterministic contact of rough surfaces J. *Tribol.* **129** pp 957-962
[10] Benchea M, Iovan-Dragomir A, Crețu S 2014 Misalignment effects in cylindrical roller bearings *App. Mech. and Mat.* **658** pp 277-282
[11] Crețu S, Benchea M, Iovan-Dragomir A 2016 On basic reference rating life of cylindrical roller bearings. Part II - Elastic-Plastic Analysis *J. Balk. Tribol. Assoc.* **22/1** pp 272-280
[12] Chaboche JL 2008 A review of some plasticity and viscoplasticity constitutive theories *Int. J. Plasticity* **24** pp 1642-1693
[13] Besson J, Cailletaud G, Chaboche JL, Forest S and Blétry M 2010 *Non-linear mechanics of materials* (Springer)
[14] ISO 16281:2008, Rolling bearings-methods for calculating the modified reference rating life for universally loaded bearings
[15] Linares Arregui I Alfredsson B 2010 Elastic-plastic characterization of a high strength bainitic roller bearing steel - experiments and modelling *Int. J. Mech. Sci.* **52** pp 1254-1268
[16] ISO 281:2007, Rolling bearings-Dynamic load ratings and rating life
[17] SKF Group 2013 *Rolling bearings catalogue*